

Glypican-3 as a potential hepatocellular carcinoma peptide vaccine candidate for the Indonesian population

Angelika¹ , Arli Aditya PARIKESIT^{2*} , Michael JONATHAN¹ , Nadya Marcelina JULIANTO¹ 

¹ Department of Biomedicine, School of Life Sciences, Indonesia International Institute for Life Sciences, Jakarta 13210, Indonesia.

² Department of Bioinformatics, School of Life Sciences, Indonesia International Institute for Life Sciences, Jakarta 13210, Indonesia.

* Corresponding Author. E-mail: arli.parikesit@i3l.ac.id (A.P.); Tel. + [+6221 295 67 888](tel:+622129567888)

Received: 21 February 2022 / Revised: 22 April 2022 / Accepted: 23 April 2022

ABSTRACT: Hepatocellular carcinoma (HCC) is the third most common cancer-related death worldwide, including in Indonesia. However, to date, there is still no effective treatment. As immunotherapy has gained more attention, this study aims to develop a peptide vaccine derived from GPC3. NetCTLPan1.1 and NetMHCPan were utilized to discover GPC3 based CTL and HTL epitopes, respectively. The peptide sequence was analyzed for its immunogenicity, IFN γ inducing capabilities, and population coverage; six-strong peptide candidates were chosen to create the vaccine. The 3D structure of the peptide vaccine was predicted using RaptorX, refined using GalaxyWEB, and then evaluated for the Ramachandran favored score using SwissProt ExPasy before being docked. A peptide vaccine of GPC3-derived peptide was constructed and proven to have potent immunogenicity, antigenicity, and population coverage. Docking results using the 3D structure against different HLA alleles reveal promising interactions, thus predicted to be able to induce T cell response. The peptide vaccine is highly potential as an alternative treatment for HCC, but further in vitro and in vivo studies should be performed to confirm these findings.

KEYWORDS: Hepatocellular carcinoma; vaccine; Indonesia; glypican-3; in silico.

1. INTRODUCTION

Over the past few years, the growing incidence of liver cancer has been a global concern. Liver cancer is currently the sixth most common cancer and the third most frequent cause of cancer-related deaths worldwide, with around 905,000 new cases and 830,000 deaths in 2020 [1]. Cancer that arises from liver cells is classified into different types, but hepatocellular carcinoma or HCC is the most commonly found primary liver malignancy. HCC is mainly caused by viral infections such as Hepatitis B (HBV) and Hepatitis C (HCV). HBV leads to HCC via a direct mechanism by synthesizing an oncovirus protein called HBx, and an indirect mechanism by inducing injury to the liver [2]. Meanwhile, HCV mostly leads to liver injury followed by cirrhosis and the development of liver cancer [2]. The second most common etiology is mycotoxin as secondary metabolites produced by fungi. An example of mycotoxin is aflatoxin B1 by *Aspergillus flavus*, a DNA intercalating factor that further leads to mutation and carcinogenesis [3]. In addition, lifestyle factors including diet, obesity, alcohol abuse, and smoking also contribute to HCC [4-5].

Currently, the major modalities used to detect HCC are utilization serum alpha-fetoprotein (AFP) as a biomarker, diagnostic imaging with either PET (Positron emission tomography) scan or CT (computerized tomography) scan, ultrasound, and magnetic resonance imaging (MRI) [6]. Unfortunately, despite the various means to diagnose HCC, most patients experience diagnostic delays either due to providers failing to identify positive tests, insensitive diagnostic tests, or patients missing surveillance appointments [6-7]. In conjunction

Angelika, Parikesit AA, Jonathan M, Julianto NM. Glypican-3 as Potential Hepatocellular Carcinoma Peptide Vaccine Candidates for the Indonesian Population. J Res Pharm. 2022; 26(4): 962-979.

with diagnostic delay is poor HCC prognosis; even delays for three months allow significant tumor growth, lowering the possibility of effective treatment alternatives [7].

Hepatitis B vaccination and blood donor screening are both effective primary preventive strategies. The impact of the mass immunization campaign on HBV-related HCC in young people will be evident shortly, with an estimated 80% reduction in HCC in adults in three to four decades [8]. Apart from that, HCC also has various types of treatment, which vary depending on the staging of the disease and associated comorbidities. There are five main treatments of HCC, including surgical removal, percutaneous ablation, radiofrequency ablation, various embolization such as transarterial chemoembolization (TACE), and radioembolization [9]. Each type of treatment has its advantages, side effects, and challenges. For instance, problems such as recurrence and metastasis of the disease may still be encountered in surgical resection and liver transplantation treatment. Besides that, there is also a limited number of donors for liver transplantation, which adds another challenge for this type of treatment [10]. Meanwhile, chemoembolization treatment has a risk of bleeding or infection of the blood vessels [11]. Apart from that, there are also some significant complications after percutaneous ablation treatment, such as hemorrhage, liver failure, portal vein thrombosis, etc. [12]. Lastly, molecular therapies still have some challenges in developing biomarkers that can predict a patient's response [13].

Immunotherapy is a popular approach to tackle this problem. Among immunotherapies is the peptide vaccine, which applies a short peptide sequence that can activate the immune system to target cancer cells. Many peptide vaccines derived from neoantigen have been developed, and the clinical trials have shown mixed results. However, neoantigen derived from the mutated gene, thus rarely detected in HLA from HCC and other types of cancer with low or intermediate mutation burden. This makes targeting neoantigen more suitable as personalized medicine instead of a wider population [14].

It is known that tumor cells express the same tumor-associated antigen (TAAs). A short 9-mer to 15-mer peptide sequence from the TAA is able to induce immunological response [15]. Based on this principle, scientists are drawn to target the TAAs by using peptide vaccines. The peptide vaccine will be processed by MHC class I and MHC class II molecules of professional antigen-presenting cell (APC), thus inducing CD8+ and CD4+ T cell response against the tumor cells. Moreover, unlike neoantigen peptide vaccines, TAAs expression profiles are primarily similar across the same type of cancer, in this case, HCC. Thus, the probability of the peptide sequence to be recognized by immune cells is bigger [14].

Hence, the proposed vaccine utilized a very well-known tumor-specific antigen, Glypican-3 (GPC3). It is an oncofetal HCC antigen that belongs to a family of cell surface heparan sulfate proteoglycans bound to the cell membrane by a glycosyl-phosphatidylinositol anchor. It is highly expressed during embryogenesis and organ development [16] but not in the adult liver [17]. However, a study by Wu, et al. [18] found that GPC3 is overexpressed in HCC patients and is associated with poor prognosis in HCC patients. Moreover, GPC3 has been found to promote the growth of HCC by activating the canonical pathway of WNT [19]. The normal WNT signaling pathway starts with the binding of WNT to frizzled (FZD). GPC3 can interact with WNT to increase WNT concentration near the cell membrane so that WNT can interact with FZD. A series of downstream signaling cascades will happen and result in the transcription of genes responsible for tissue renewal and regeneration in adults [20]. Interestingly, another study by Capurro et al. in 2014 [20], found that GPC3 can also directly bind to FZD as well. Several previous studies have managed to create promising vaccines for HCC, which included GPC-3 as the chosen antigen [21-23]. This further supports the rationale behind selecting this antigen for the in-silico peptide vaccine design for HCC designated for the Indonesian population.

In this study, peptides derived from GPC3 are the peptides of interest that were further investigated to predict epitope candidates for designing an HCC vaccine specific to the Indonesian HLA allele. These peptides were examined through immunoinformatics approaches to investigate the Indonesian HLA class I and class II binding epitopes, peptide immunogenicity, population coverage, and self-peptide analysis. Furthermore, the candidates were combined into a single polypeptide, and the 3D structure was predicted. The molecular docking was also performed to analyze the interaction between GPC3 peptide and HLA molecule.

2. RESULTS

2.1. Identification of HLA allele frequencies in Indonesia

The allele frequencies commonly found in Indonesia are obtained from the Allele Frequency Net Database. The obtained 20 hits of alleles for both MHC class I and II that can be found in Indonesia are listed in **Table 1**. The top 5 allele frequencies found for both MHC class I and II are HLA-A24:07 (22.2%), HLA-A11:01 (16.4%), HLA-A33:03 (16.2%), HLA-A24:02 (13.9%) and HLA-DRB 07:01 (13.6%). The highest allele frequency, HLA-A24:07 is crucial especially for Javanese population.

2.2. Predicted T and B cells epitopes of GPC3 antigen

Both CTL and HTL epitopes of GPC3 that bind to HLA class I and HLA class II epitopes were predicted using NetCTLpan1.1 and NetMHCIIpan-4.0, respectively. Class I immunogenicity analysis was performed after the epitopes were discovered. **Table 2** shows various CTL epitopes bind strongly to HLA class I with the corresponding immunogenicity. Out of 56 HLA-epitope binders, 30 have a positive immunogenicity score, which means it is most likely to produce CTL response when introduced in vitro. The peptide was sorted from the highest immunogenicity score (0.38167) to the lowest (0.00585). Peptide with strongest immunogenicity was discovered to bind to HLA-A02:01.

Meanwhile, potential HTL binds to HLA class II with strong affinity was also discovered. Epitopes were also assigned to the IFN epitope server to predict whether they are able to induce the production of IFN γ or not. The listed peptide epitopes that are positive for IFN γ were shortlisted at **Table 3**. The peptides were sorted from the highest IFN- γ score to the lowest. Peptide with the highest IFN- γ score was identified as HLA-DRB11:01 binders. The antibody epitope prediction is made to predict B-cell epitopes from the GPC3 (**Figure 1**). The prediction was made using the IEDB analysis tool with Bepipred linear epitope prediction 2.0 method. Here, the yellow area indicates the sequence in GPC3 that has a score above the 0.5 threshold, which further indicates that the sequence is able to bind to antibodies. The longest sequence (86 aa) predicted to bind to the antibody was position 497R to 582H. Meanwhile, the highest score of the antibody epitope prediction is still above the 0.5 threshold, which is 0.658.

2.3. Population coverage analysis of the epitopes

The population coverage was obtained from IEDB utilizing the epitope obtained from the binding prediction server for both MHC class I and II allele. A total of three CTL epitopes (QAFEFVGEF, KYPIFFLCI, and AYPEDLFI) and three HTL epitopes (FEIVVRHAK, IVVRHAKNY, and FLIIQNAAV) were chosen for further population coverage analysis for Javanese and Sundanese-Javanese population. The result in **Table 4** shows that the coverage of the alleles is very high, reaching 97.53% Observed separately, Class I and Class II coverage is also quite high, reaching 84.32% and 84.28%.

2.4. Construction and evaluation of the GPC3 based peptide vaccine

The GPC3 based peptide vaccine construct consists of three CTL epitopes (QAFEFVGEF, KYPIFFLCI, and AYPEDLFI) and three HTL epitopes (FEIVVRHAK, IVVRHAKNY, and FLIIQNAAV) that were selected due to their high immunogenicity and IFN score. Furthermore, several epitopes in the construct also had the capability to bind to HLA-A_{24:02} and HLA-A_{24:07}, which are unique Indonesian HLA. The CTL epitopes were linked by the AAY linkers, while the HTL epitopes were merged by the GPGPG linkers. Aside from the epitopes, two types of adjuvants, human β -defensin-3 and TAT sequence, were also added into the construct to elevate the vaccine's immunogenicity. The human β -defensin-3 sequence was fused into the N-terminal of the vaccine construct with the aid of an EAAAK linker. Lastly, the TAT sequence was linked by the GPGPG linker to the C-terminal of the vaccine construct (**Figure 2**). Following the construction, the vaccine also underwent an antigenicity test, and the prediction score obtained was 0.5531, where it is able to induce antigenic response as a probable antigen.

2.5. Peptide 3D Modeling

The 3D modeling of the construct selected in the previous step was put into a RaptorX server. The server predicts the 3D structure of the constructed peptide using deep learning. Several 3D models were suggested by the tool. The model that ranked first based on the suggestion was chosen, which is depicted in **Figure 3**, with an estimated root mean square deviation (RMSD) of 7.4113.

To further refine the 3D model, the 3D model was put into a GalaxyWEB server. Five different models were suggested (**Table 5**) by the server, and model 5 was chosen, having a high Rama favored score of 92 compared to the other models. The GDT-HA (global distance test - high accuracy) score of models 5 is 0.9375 out of a maximum of 1, which corresponds to maximum accuracy.

The MolProbity analysis using the SwissProt ExPasy server (**Table 6**) resulted in a Ramachandran favored score of 91.98% and a MolProbity Score of 2, in line with the Molprobity and Rama favored score in GalaxyWEB. No rotamer outliers were detected in the SwissProt analysis, similar to the result from GalaxyWEB. The Ramachandran plot is illustrated in **Figure 4**. The plot shows that most of the residues of the vaccine construct fall into the allowed/favored regions. However, some of the residues are considered outliers, such as A107 PRO, A97 VAL, A67 PHE, A63 LYS. While there are no bad bonds, 32 residues were identified to form bad angles, all of which are listed in **Table 6**.

2.5. Molecular docking of the vaccine construct

The Cluspro 2.0 server was used to dock the vaccine construct Model 5 with the most frequent HLA found in Indonesia, including HLA-A*11:01, A*24:02, B*35:05, and B*15:02 (**Table 7**). It is discovered that interactions between Model 5 and HLA-B*35:05 have the lowest energy weighted score of -1058.4. The strongest interaction occurred at LYS63 residue of Model 5 against THR233 of HLA-A*11:01, with LYS63 as the H-donor (1.6525 Å). Apparently, this interaction is also observed between Model 5 and HLA-B*35:05 and B*15:02. The docked complexes were then visualized (**Figure 5**). It seems that a similar hydrophobicity profile was present in the binding sites of Model 5 to HLA molecules.

Table 1. The most common HLA allele in Indonesia and its frequency.

HLA Alleles	Population	Allele Frequency
A*02:01	Indonesia Java-Western	0.0660
A*11:01	Indonesia Java-Western	0.1640
A*24:02	Indonesia Java-Western	0.1390
A*24:07	Indonesia Java-Western	0.2220
A*33:03	Indonesia Java-Western	0.1620
A*34:01	Indonesia Java pop 2	0.0830
A*34:01	Indonesia Java-Western	0.0730
A*34:01	Indonesia Sundanese and Javanese	0.0670
B*15:02	Indonesia Java Western	0.1220
B*15:13	Indonesia Java-Western	0.1150
B*15:21	Indonesia Java-Western	0.0730
B*18:01	Indonesia Java-Western	0.0640
B*35:05	Indonesia Java-Western	0.0860
B*38:02	Indonesia Java-Western	0.0540
B*44:03	Indonesia Java Western	0.0930
B*58:01	Indonesia Java Western	0.0590
DRB1*07:01	Indonesia Java Western	0.1360
DRB1*11:01	Indonesia Nusa Tenggara Island	0.0890
DRB1*12:02	Indonesia Java Western	0.3650
DRB1*15:02	Indonesia Java Western	0.2330

Table 2. The predicted peptides that bind to HLA class I.

No	Peptide	HLA Allele	Immunogenicity
1	FVGEFFTDV	HLA-A*02:01	0.38167
2	QAFEFVGEF	HLA-B*15:02, HLA-B*15:13, HLA-B*15:21, HLA-B*35:05	0.37871
3	AHVEHEETL	HLA-B*38:02	0.34708
4	KYPIFFLCI	HLA-A*24:02, HLA-A*24:07	0.31366
5	ISVVCFFFL	HLA-B*58:01	0.27984
6	SVVCFFFLV	HLA-A*02:01, HLA-A*34:01	0.27567
7	NQLRFLAEL	HLA-B*38:02	0.24356
8	HFKYPIFFL	HLA-A*33:03	0.20796
9	LRFLAELAY	HLA-B*18:01	0.17269
10	AYYPEDLFI	HLA-A*24:02, HLA-A*24:07	0.16506
11	GEFFTDVSL	HLA-B*18:01, HLA-B*38:02, HLA-B*44:03	0.15266
12	FDSLFPVIY	HLA-B*18:01	0.1513
13	FLAELAYDL	HLA-A*02:01, HLA-A*38:02	0.14932
14	EVINTTDHL	HLA-A*34:01	0.14865
15	YWREYILSL	HLA-A*24:02	0.1332
16	LFPVIYTQL	HLA-A*24:02, HLA-A*24:07	0.12914
17	VINTTDHLK	HLA-A*11:01	0.11646
18	FLIIQNAAV	HLA-A*02:01	0.11411
19	STFHNLGNV	HLA-A*34:01	0.07863
20	KSLQVTRIF	HLA-B*58:01	0.07802
21	FPVIYTQLM	HLA-B*35:05	0.07602
22	AELAYDLDV	HLA-B*44:03	0.05665
23	NEISTFHNL	HLA-B*18:01, HLA-B*38:02, HLA-B*44:03	0.04825
24	HQVRSFFQR	HLA-A*33:03	0.0457
25	RTACLVVAM	HLA-B*58:01	0.04421
26	VAENDTLCW	HLA-B*58:01	0.04327
27	MENVLLGLF	HLA-B*18:01, HLA-B*44:03	0.04032
28	LIQNAAVF	HLA-B*15:02, HLA-B*15:13, HLA-B*15:21, HLA-B*35:05	0.01431
29	VLLGLFSTI	HLA-A*02:01	0.01296
30	KIWHFKYPI	HLA-A*02:01	0.00585

2.6. Self-peptide Analysis

The vaccine construct exhibited no similarities to human peptides apart from the human β -defensin protein that was intentionally put into the construct as an adjuvant to trigger an immune response (Figure 6).

3. DISCUSSION

3.1. Vaccine Construction

Human Leukocyte Antigen (HLA) are highly polymorphic, even known to be the most polymorphic gene in humans. Different individuals would have different alleles, and they are even more varied in Indonesia, where the population is enormous while the people are divided into countless ethnic, race, and

cultural groups [24]. Unfortunately, the highly polymorphic HLA allele becomes the limitation in making peptide-based vaccines as not all peptides are able to bind specific HLA molecules [25-26]. Nonetheless, as can be seen in **Table 1**, several HLA alleles are more common than the others. Designing a vaccine using peptides that are restricted to these common HLA molecules could increase the population coverage (**Table 3**).

Net-CTLPan1.1 predicted the binding of 9 mer peptides from GPC3 to HLA class I molecules. Strong binders are most likely to induce CD8+ cells immune response, which is very important in eliminating tumor cells [27]. The prediction algorithm includes three main parameters: peptide binding to MHC class I, proteasomal C-terminal cleavage, and TAP (transporter associated with antigen processing) transport. In order to further exclude non-immunogenic peptides, the strong binders from Net-CTLPan1.1 were subjected to another analysis with Class I Immunogenicity prediction tools from IEDB. It turns out not all strong binders have strong immunogenicity (**Table 2**).

Meanwhile, GPC3 peptides bound to HLA class II were predicted using Net-MHCPan-4.0 (**Table 3**). Similar to Net-CTLPan1.1, this software also involves peptide processing aside from the binding affinity. Although many cancers immunotherapy focuses more on CD8+ T cells, a study has shown that CD4+ T cells also play important roles mainly by activating CD8+ T cells, direct antitumor immunity achieved by the production of IFN- γ and TNF- α , and activating antibody-producing B cells [28]. Aside from triggering direct antitumor immunity, IFN- γ helps differentiate naive T cells into CD8+ T cells and aids in their proliferation. Moreover, IFN- γ induces the "classical" polarization of macrophages towards those with a proinflammatory profile [29]. These summarized why predicting the ability of peptide sequence to induce IFN- γ is crucial in vaccine construction.

Table 3. The predicted peptides that bind to HLA class II.

No	Peptide (15 mer)	Peptide (9 mer)	HLA	IFN score
1	VFQEA FEIVVRHAKN	FEIVVRHAK	HLA-DRB*11:01	0.99709285
2	FQEA FEIVVRHAKNY	FEIVVRHAK	HLA-DRB*11:01	0.95512342
3	EAFEIVVRHAKNYTN	FEIVVRHAK	HLA-DRB*11:01	0.74654834
4	EAFEIVVRHAKNYTN	IVVRHAKNY	HLA-DRB*12:02	0.74654834
5	QEAFEIVVRHAKNYT	FEIVVRHAK	HLA-DRB*11:01	0.64504629
6	QEAFEIVVRHAKNYT	IVVRHAKNY	HLA-DRB*12:02	0.64504629
7	LKFLIIQNAAVFQEA	FLIIQNAAV	HLA-DRB*15:02	0.57449334
8	ELKFLIIQNAAVFQE	FLIIQNAAV	HLA-DRB*07:01, HLA-DRB*15:02	0.55791633
9	MELKFLIIQNAAVFQ	FLIIQNAAV	HLA-DRB*15:02	0.55617682
10	A FEIVVRHAKNYTNA	IVVRHAKNY	HLA-DRB*12:02	0.26649461
11	ELIQKLSFISFYSA	LKSFISFYS	HLA-DRB*15:02	0.23274713
12	LIQKLSFISFYSA	LKSFISFYS	HLA-DRB*15:02	0.22835791
13	MEEKYQLTARLNMEQ	YQLTARLNM	HLA-DRB*11:01	0.22034221
14	LKSFISFYSA LPGA	ISFYSA LPGA	HLA-DRB*15:02	0.12309987
15	DNEISTFHNLGNVHS	ISTFHNLGN	HLA-DRB*15:02	0.094234149
16	LNMEQLLQSASMELK	LLQSASMEL	HLA-DRB*07:01	0.08392476
17	SMELKFLIIQNAAVF	FLIIQNAAV	HLA-DRB*15:02	0.070282914
18	RRRELIQKLSFISF	IQKLSFIS	HLA-DRB*12:02	0.069624799
19	KSFISFYSA LPGA	ISFYSA LPGA	HLA-DRB*15:02	0.050873904
20	RELIQKLSFISFY	IQKLSFIS	HLA-DRB*12:02	0.034590432
21	KLKSFISFYSA LPGA	ISFYSA LPGA	HLA-DRB*15:02	0.024479533
22	KVKNQLRFLAELAYD	LRFLAELAY	HLA-DRB*12:02	0.017517663
23	RRELIQKLSFISFY	IQKLSFIS	HLA-DRB*12:02	0.0083627795

Apart from T cells, B cells activation is also crucial for anti-tumor immunity. B cells secrete immunoglobulins (Ig) which inhibit tumor growth [30]. Additionally, B cells promote T cells response by

aiding through the antigen presentation process. Another role of B cells that are mostly ignored is suppressing pro-tumorigenic cells called Bregs. Bregs produce cytokines such as IL-10, TGF- β , and STAT3, which suppress NK and T cell response [31]. These factors also support MDSC, which further suppresses the anti-tumor immune response in the tumor microenvironment [32].

As a result, a peptide-based vaccine approach was applied in this study. A peptide-based vaccine is one of the active cancer immunotherapies that functions to evaluate both innate and adaptive immune responses against tumor-specific or associated antigens [33]. This approach is prominent in cancer treatment due to its advantages, including high specificity, safety, cost-efficient production, and stability. However, peptide-based vaccines, especially single-epitope-based vaccines, may possess low immunogenicity and rapid degradation [34].

Therefore, two types of adjuvants, human β -defensin-3 and TAT sequence, were fused with the epitopes from GPC3 to enhance the immunogenicity of the peptide-based vaccine further. The human β -defensin-3 was linked to the N-terminal, while the TAT sequence was connected to the C-terminal of the vaccine construct. The human β -defensin-3 is able to interact with chemokine receptor-6 (CCR-6), which elicits innate immune responses. Not to mention, the human β -defensin-3 is also crucial in the recruitment of naive T cells. On the other hand, the TAT sequence functions to help the vaccine construct's intracellular delivery [35]. Lastly, the epitopes and adjuvants in the GPC3-based vaccine were fused using three types of linkers (EAAAK, AAY, and GPGPG). Besides linking the epitopes, these linkers also play crucial roles in the protein folding, flexibility, and vaccine construct's stability [36]. After the GPC-3 based vaccine was constructed, the vaccine was further evaluated by using an antigenicity test to reveal the ability of the antigen in eliciting immune responses from B cell and T cell [37]. The threshold for tumor antigenicity in the Vaxijen server is set to 50%, whereas the prediction score of the GPC-3 based vaccine construct was 55,31%. Hence, the GPC-3 based vaccine construct has the potential as a vaccine to promote immune responses. The chosen peptides were different from previous peptide vaccine constructs that already undergo Phase II clinical trials in Japan [21]. The difference might be due to the difference in HLA allele between countries. As previously mentioned, Indonesian alleles are heterogenous hence the peptide was chosen based on the most commonly found HLA allele [27].

3.2. Peptide 3D Modeling

The aim of this step is to create a 3D model of the vaccine construct. This study opted to use RaptorX. It is a web server that can predict the 3D structure of a protein sequence without the help of any templates, unlike homology modeling [38]. There are several prediction software that can be utilized, such as PSIPRED [39], JPRED [40], SPINE-X [41], and SANN [42]. However, RaptorX was chosen because it had achieved the highest accuracy for secondary structure prediction [43].

RaptorX produced several models, and the number one suggested model was chosen for refinement in GalaxyWEB. Six different parameters were evaluated for every refinement model. GDT-HA measures the agreement between a predicted model and the experimental structure. The score reflects the accuracy in the placement of C α atom positions [43]. Model 5 had a score of 0.9375, which is the fourth-lowest score compared to the other models. However, model 5 had the lowest MolProbity score. Molprobity is a log-weighted combination of Clash score, percentage Ramachandran not favored, and percentage bad side-chain rotamers [44]. Therefore, a lower Molprobity score in the models provided than in the initial template put into the prediction software would be highly sought after. This is one of the reasons why model 5 was chosen. Clash score is the number of serious clashes per 1,000 atoms [44]. Therefore, a lower score would be better, which both model 5 and model 1 satisfied. However, model 1 was not selected because it had a lower GDT-HA score. All of the models did not have bad rotamers, which is good since poor rotamers are in unfavorable conformations [44]. The next parameter is the Ramachandran favored percentage. Model 5 had the highest Rama favored score of 92%, higher than the initial 3D model that was put into the refinement tool. A high Rama favored score signifies that the majority of the backbone angles of the residues are in the favored regions in the Ramachandran plot. This is in agreement with the result of the Ramachandran plot generated from the SwissProt MolProbity analysis (Table 3), whereby most of the residues are within the favored region in the Ramachandran plot. The Ramachandran plot from the SwissProt result was also similar to the GalaxyWEB analysis, which further substantiated the accuracy of the 3D model generated from RaptorX and the refinement done by GalaxyWEB. Furthermore, RaptorX has been utilized to predict the 3D structure of a peptide sequence as a vaccine for hepatocellular carcinoma [45], Kaposi sarcoma [46], and even a universal cancer vaccine [47].

Table 4. The population coverage of GPC3 based peptide vaccine in Indonesia

Antigen	Class I			Class II			Class Combined		
	Coverage ^a	Average hit ^b	pc90 ^c	Coverage ^a	Average hit ^b	pc90 ^c	Coverage ^a	Average hit ^b	pc90 ^c
GPC3	84.32%	2.03	0.64	84.28%	1.03	0.64	97.53%	3.06	1.56

^a projected population coverage

^b average number of epitope hits/ HLA combinations recognized by the population

^c minimum number of epitope hits/ HLA combinations recognized by 90% of the population

3.3 Molecular Docking

The Cluspro 2.0 server uses PIPER, a docking program that implements the Fast Fourier Transform (FFT) correlation method. FFT calculates energy function, thus enabling the sampling of billions of conformations of two interacting proteins. In Cluspro, the docked protein model was selected based on the cluster size. The bigger the cluster size, the higher probability of interactions. Furthermore, the server provides information regarding the lowest energy. It does not directly affect the binding affinity, but low-energy regions are more likely to produce more docked structures clusters [48-49].

In order to design an efficient vaccine construct based on antigen, it is crucial to properly understand the structural basis of antigen-HLA interactions. Direct and template-based docking methods are the two types of docking procedures. Direct techniques use thermodynamics to discover the structure of the target complex situated at the lowest Gibbs free energy in conformational space, which necessitates a computationally feasible free-energy evaluation model and an effective reduction algorithm [48]. The biological activity of the ligand is inferred by hydrogen bonds and hydrophobic interactions between the ligand and the particular target.

The average number of hydrophobic atoms in marketed drugs is 16, with one to two donors and three to four acceptors [50]. This emphasizes the value of hydrophobic interactions in medication development. They can improve the affinity of binding between target-vaccine interfaces. It has already been observed that inserting them at the hydrogen bonding location can improve the binding affinity and medication effectiveness related to hydrophobic interactions [51]. Figure 5 shows many hydrophobic interactions are present in the HLA-B*35:05 binding site and may be important for vaccine-HLA binding. This HLA-B*35:05 model shows promising results in both the lowest energy and hydrophobic interactions.

4. CONCLUSION

In conclusion, a vaccine composed of GPC3-derived peptides was developed in order to promote immune responses against HCC. The vaccine construct consists of six T cell epitopes obtained from GPC3, which have strong immunogenicity and high population coverage. Further analysis indicates that the vaccine construct is highly potential as a treatment against HCC, and it can cover most of Indonesian populations. Additionally, structural docking between vaccine and HLA molecules shows promising interactions, allowing the activation of CTLs. In addition, BLASTp analysis revealed that the constructed peptide vaccine exhibited no similarities to human peptides. Be that as it may, further in vitro and in vivo studies should be conducted to verify the efficacy of constructed peptide vaccines towards HCC.

5. MATERIALS AND METHODS

5.1. Protein sequence retrieval

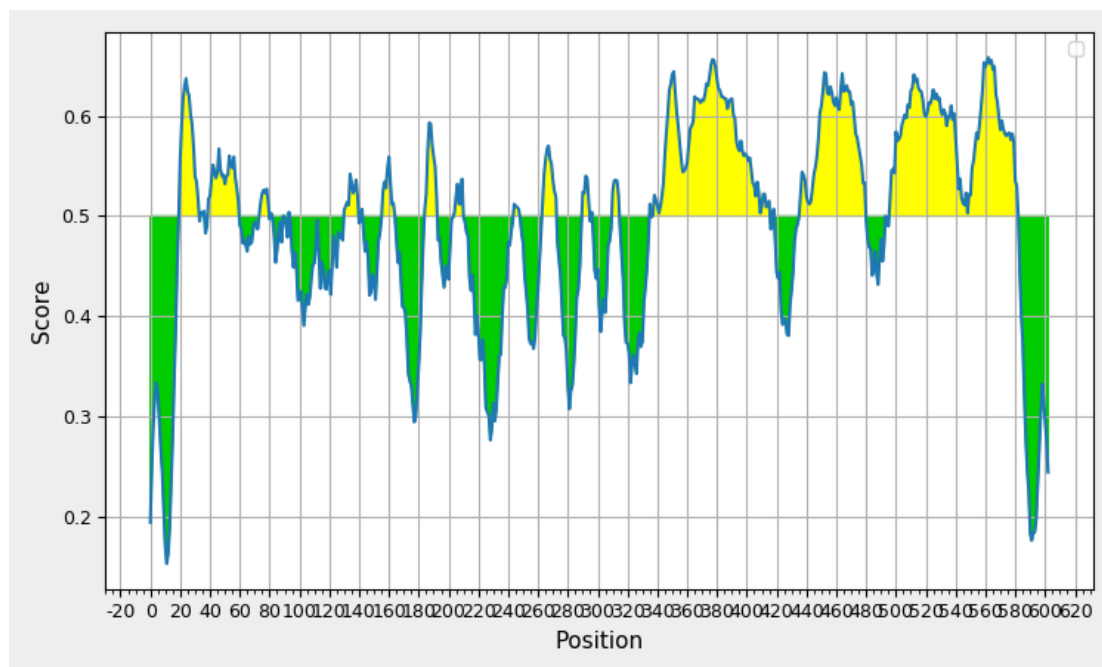


Figure 1. The antibody epitope prediction result of GPC3 antigen using the IEDB tool and Bepipred linear epitope prediction 2.0 method. The average score is 0.494, the minimum score is 0.154, and the maximum score is 0.658.

The FASTA sequence for GPC3 was retrieved from NCBI. The FASTA sequence for all of the isoforms was retrieved (NP_001158089.1; NP_001158090.1; NP_001158091.1; NP_004475.1), and the longest isoform (NP_001158089.1) was used as the target sequence.

5.2. Identification of Indonesia's allele frequencies

The Allele Frequencies Net Database (<http://allelefrequencies.net/default.asp>) was used to identify the predominant HLA alleles among the Indonesian population. The parameter "Indonesia" was selected for the country tab. Alleles that were found to have frequencies >5% of the Indonesian population were included for further analysis.

5.3. Prediction of T and B cell epitopes

The NetCTLpan - 1.1 (<https://services.healthtech.dtu.dk/service.php?NetCTLpan-1.1>) was used to predict CD8+ T-cell peptides from glypican-3 protein that will bind to MHC class I molecules. The sequence of GPC3 was inputted into the sequence tab along with Indonesia's HLA-A and HLA-B allele from the previous analysis. The threshold for C terminal cleavage was set to 0.225, while the TAP efficiency was set to 0.025. The threshold used for epitope identification was 1.0. Several 9-mer peptides with the "E" indicator were chosen as "MHC class I-binders" and validated for their immunogenicity using the class I Immunogenicity analysis tool by IEDB (<http://tools.iedb.org/immunogenicity/>).

To predict CD4+ T-cell peptides, NetMHCIIpan - 4.0 server (<https://services.healthtech.dtu.dk/service.php?NetMHCIIpan-4.0>) was used. The sequence of GPC3 and Indonesia's HLA-DRB1 alleles was inputted. The thresholds for strong and weak binding were set to 2% and 10%, respectively. Several peptides with the "SB" indicator were chosen as "MHC class II-binders". Their IFN γ -inducing capabilities were evaluated using an IFN γ epitope prediction tool (<http://crdd.osdd.net/raghava/ifnepitope/predict.php>).

The last prediction to be done was the B-cell epitope. The antibody prediction epitope tool by the Immune Epitope Database and Analysis Resource (IEDB) (<http://tools.iedb.org/bcell/>) was used to predict B-cell epitopes of glypican-3 protein. The sequence of GPC3 was inputted in the sequence tab, and the Bepipred Linear Epitope 2.0 was chosen as the method.

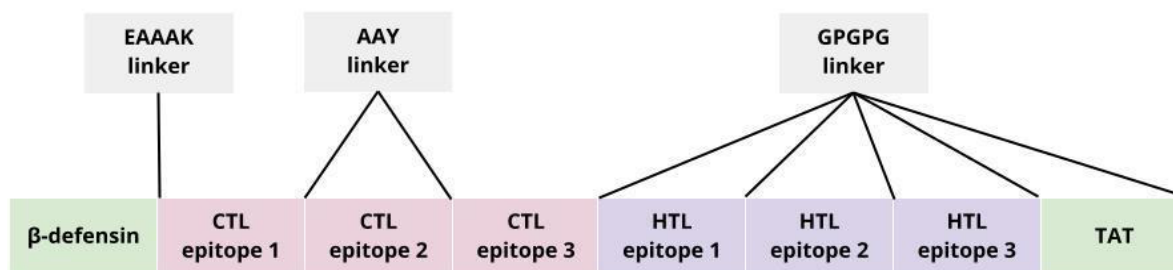


Figure 2. The schematic diagram of the GPC3 based peptide vaccine.

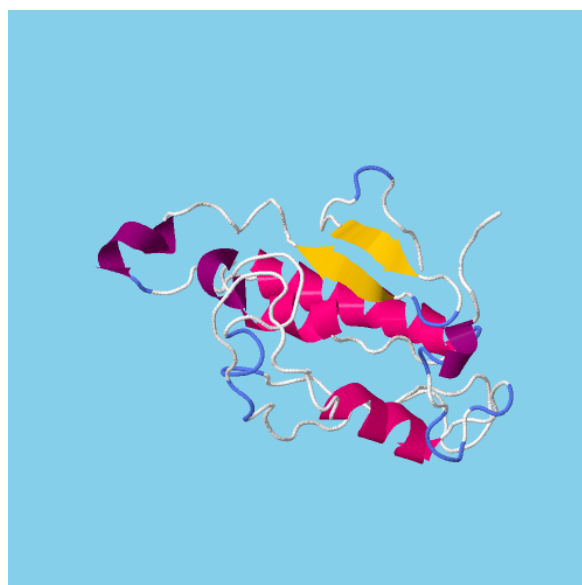


Figure 3. The predicted 3D structure of the vaccine that was constructed from RaptorX.

Table 5. The protein structure refinement of models in GalaxyWEB. GDT-HA: global distance test - high accuracy; RMSD: root-mean-square deviation.

Model	GDT-HA	MolProbity	Clash Score	Poor rotamers	Rama favored
Initial	1	2.687	24.6	1.7	86.4
Model 1	0.9253	2.201	15.5	0	91.4
Model 2	0.9436	2.268	17.4	0	90.7
Model 3	0.9405	2.221	16.3	0	91.4
Model 4	0.9421	2.211	15.9	0	91.4
Model 5	0.9375	2.180	15.5	0	92.0

5.4. Population coverage analysis and vaccine construct design

A series of CD8⁺ and CD4⁺ epitopes was chosen as the construct. In order to evaluate the construct, a population coverage analysis using the IEDB Population Coverage tools (<http://tools.iedb.org/population/>) was conducted. The epitopes of GPC3 were inputted, and the country parameter tab was set to Indonesia. A

group of peptides with high coverage ($\geq 90\%$) was chosen. Linkers and adjuvants were also included between the included epitopes.

Table 6. The MolProbity analysis of Model 5 using SwissProt.

MolProbity Results		GDT-HA
MolProbity score	2	
Clash Score	9.74	
Ramachandran favored	91.98%	
Ramachandran outliers	2.47%	A107 PRO, A97 VAL, A67 PHE, A63 LYS
Rotamer outliers	0	
C-beta deviations	8	
Bad bonds	0/1265	
Bad angles	32/1709	A90 PHE, (A62 TYR-A63 LYS), A9 TYR, A140 PHE, A76 TYR, A82 PHE, A67 PHE, A59 PHE, A97 VAL, A77 TYR, A78 PRO, A132 LEU, A53 PHE, A63 LYS, (A101 ALA-A102 LYS), A117 HIS, A99 ARG, (A82 PHE-A83 ILE), A136 ASN, A100 HIS, (A111 PHE-A112 GLU), A96 ILE, A17 ARG, (A96ILE-A97 VAL), A143 ALA, (A66 ILE-A67 PHE)

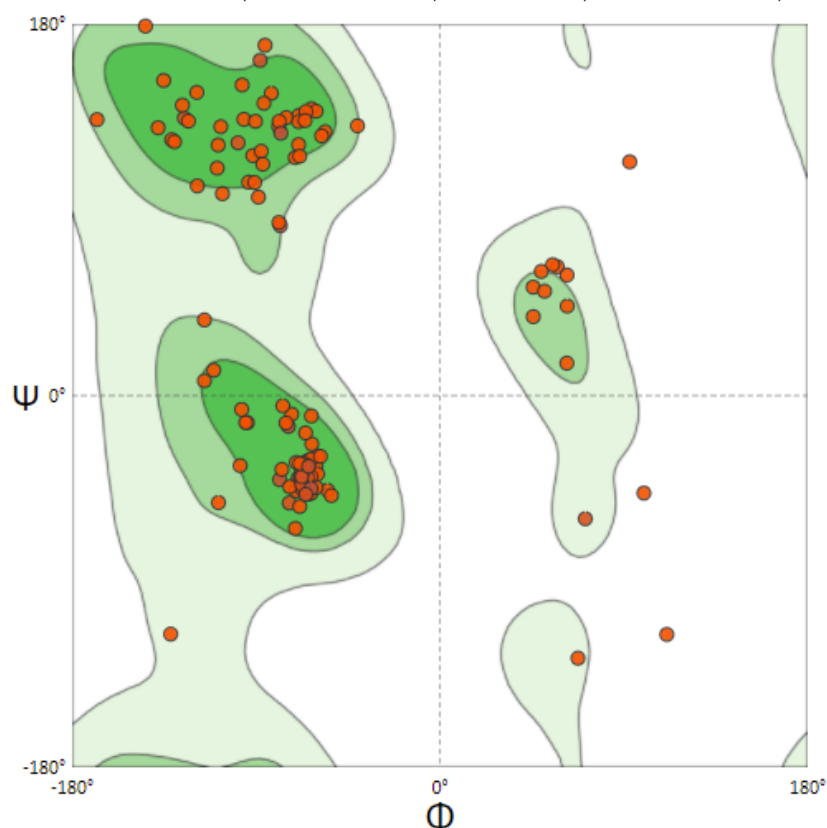


Figure 4. The Ramachandran plot of Model 5. The green-colored areas are the allowed regions and the orange dots are the residues of the vaccine construct. Most of the residues fall within the allowed/favored regions.

Table 7. Summary of molecular interactions of the vaccine construct against HLA class I.

HLA	Lowest Energy	Hydrogen bond Interactions			
		Complex Pair		Interacting Atoms	Bond Distance (Å)
		Peptide	HLA		
A*11:01	-959.4	ARG21	PRO105 HH11	O - H	2.07971
		ARG21	PRO105 HH21	O - H	1.94027
		THR5	THR190	O - H	1.88498
		LEU6	HIS192	O - H	2.15465
		CYS11	ARG202 HH11	O - H	1.92504
		GLN7	ARG202	O - H	1.76041
		CYS11	ARG202 HH21	O - H	1.96329
		VAL13	LEU230	O - H	2.97056
		ARG234 HH11	GLY1	O - H	2.15229
		ARG234 HH21	GLY1	O - H	1.74023
		THR5	HIS188	H - N	2.41295
		GLN7	HIS192	H - N	2.583
		TYR10	THR200	H - O	1.85173
		ARG12	ASP227	H - O	2.60818
		VAL13	GLU229	H - O	2.12593
		LYS63	THR233	H - O	1.6525
A*24:02	-976.6	PRO147	THR10	O - H	2.13605
		GLY144	ARG21 HH11	O - H	2.54416
		GLY146	ARG21 HH11	O - H	2.46411
		ALA143	ARG21 HH12	O - H	2.76424
		GLY146	ARG21 HH21	O - H	1.98349
		ALA158	GLN96 HE22	O - H	2.08371
		TYR10	ARG202 HE	O - H	2.159
		TYR10	ARG202 HH22	O - H	1.78144
		VAL13	GLU232 H	O - H	2.31917
		CYS11	ARG234 HH11	O - H	2.55869
		CYS11	ARG234 HH12	O - H	2.96766
		ILE3	ARG234 HH21	O - H	2.38587
		GLN7	ARG234 HH21	O - H	2.39489
		GLY1	GLN242 HE22	O - H	1.90903
		GLN7	TRP244 HE1	O - H	2.02207
		TYR10	GLU229	H - O	1.89603
		ARG17	GLN96	H - O	2.24075
		LYS26	HIS192	H - O	1.89434
		GLY160	GLY120	H - O	2.79202

Table 7. Summary of molecular interactions of the vaccine construct against HLA class I (Continued).

HLA	Lowest Energy	Hydrogen bond Interactions			
		Complex Pair		Interacting Atoms	Bond Distance (Å)
		Peptide	HLA		
B*35:05	-1058.4	GLY106	ARG35 HH12	O - H	2.3801
		TYR62	ARG48 HH21	O - H	1.75561
		PRO147	GLN96 HE21	O - H	2.3531
		LEU6	HIS192 HD1	O - H	2.4027
		TYR10	ARG202 HH11	O - H	1.8298
		TYR10	ARG202 HH21	O - H	1.88426
		THR5	TRP204 HE1	O - H	2.54504
		VAL13	GLU232 H	O - H	2.66484
		GLN7	TRP244 HE1	O - H	2.03719
		TYR10 HH	THR200	H - O	2.75285
		ARG12 HE	GLU229	H - O	1.91938
		LYS63	THR233	H - O	1.69116
		B*15:02	-954.9	GLY150	THR10
GLU142	ARG21			O - H	1.80645
ALA143	ARG21			O - H	2.23496
PRO145	GLN32			O - H	2.44916
PRO145	ARG35			O - H	1.76209
PRO105	ARG35			O - H	1.95654
GLY106	ARG48			O - H	1.89418
PRO107	ARG48 HH11			O - H	1.92646
PRO107	ARG48 HH21			O - H	2.1181
LEU6	HIS192			O - H	2.12021
GLN7	ARG202			O - H	1.72814
TYR10	ARG202			O - H	1.75839
THR5	TRP204			O - H	3.0826
VAL13	GLU232			O - H	2.1317
GLY1	ARG234 HE			O - H	2.64079
GLY1	ARG234 HH22			O - H	1.9615
TYR10	GLU229			H - O	1.97158
ARG12	GLU229			H - O	1.92493
ALA19	GLU232			H - O	2.13841
LYS63	THR233	H - O	1.69433		

5.5. Construct Antigenicity analysis

Vaxijen (<http://www.ddg-pharmfac.net/vaxijen/VaxiJen/VaxiJen.html>) was used to evaluate the antigenicity of the construct. The construct was carried on to the next step of the analysis if it had a score of ≥ 0.5 .

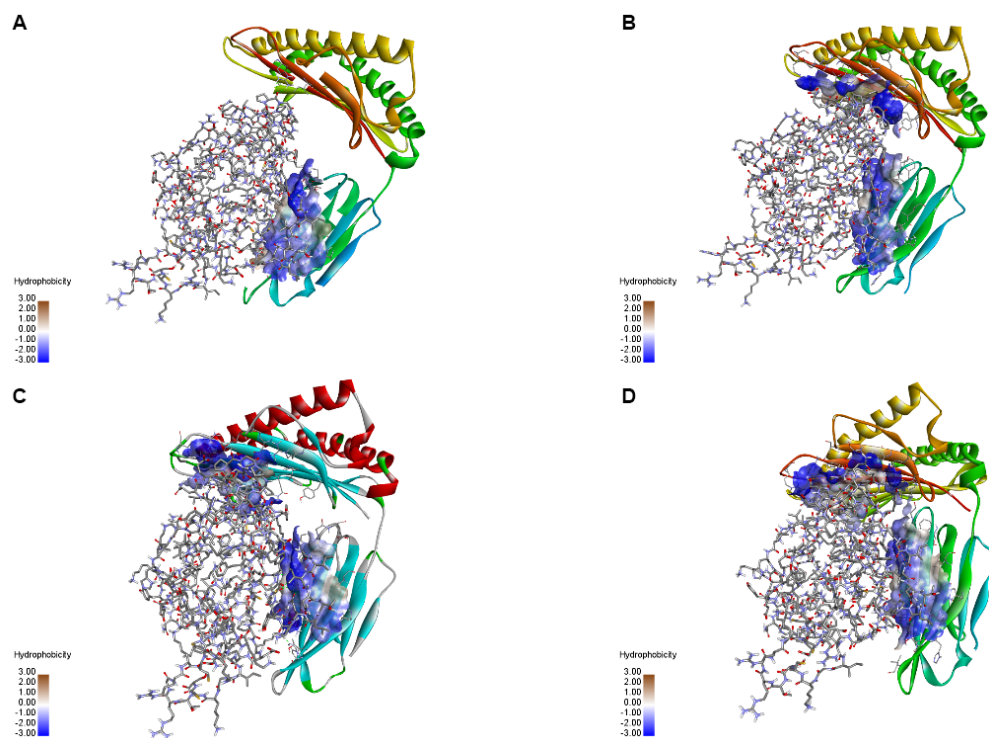


Figure 5. Comparison of hydrophobicity docking (binding) sites of (a) A*11:01, (b) B*15:02, (c) A*24:02 and (d) B*35:05 on Model 5. The residues at the interface are represented as lines and sticks. H-bonds (green color) between two molecules are displayed using a dashed line.,

i Your results are filtered to match records that include: Homo sapiens (taxid:9606)

Job Title	Protein Sequence
RID	5R90N5YR016 <small>Search expires on 04-18 13:22 pm</small> Download All ▼
Program	BLASTP Citation ▼
Database	nr See details ▼
Query ID	lcl Query_37889
Description	unnamed protein product
Molecule type	amino acid
Query Length	164
Other reports	Distance tree of results Multiple alignment MSA viewer ?

Filter Results

Organism only top 20 will appear exclude
 Homo sapiens (taxid:9606)
[+ Add organism](#)

Percent Identity to
E value to
Query Coverage to

[Filter](#) [Reset](#)

Descriptions | [Graphic Summary](#) | [Alignments](#) | [Taxonomy](#)

Sequences producing significant alignments [Download](#) ▼ [Select columns](#) ▼ Show ?

select all 4 sequences selected [GenPept](#) [Graphics](#) [Distance tree of results](#) [Multiple alignment](#) [MSA Viewer](#)

Description	Scientific Name	Max Score	Total Score	Query Cover	E value	Per. Ident	Acc. Len	Accession
<input checked="" type="checkbox"/> beta-defensin_3 [Homo sapiens]	Homo sapiens	75.1	75.1	21%	1e-14	100.00%	45	AAV41025.1
<input checked="" type="checkbox"/> beta-defensin-like protein [Homo sapiens]	Homo sapiens	75.1	75.1	21%	2e-14	100.00%	77	ACK99045.1
<input checked="" type="checkbox"/> beta-defensin_103 precursor [Homo sapiens]	Homo sapiens	74.7	74.7	21%	3e-14	100.00%	67	NP_001075020.1
<input checked="" type="checkbox"/> beta-defensin-3 [Homo sapiens]	Homo sapiens	70.1	70.1	21%	1e-12	97.14%	67	AAM62424.1

Figure 6. The self-peptide analysis in BLASTp using the peptide vaccine sequence.

5.6. Peptide 3D Modelling and Molecular Docking

The way the small peptide folds and forms a 3D structure was predicted using the RaptorX server (<http://raptorx.uchicago.edu>). The sequence was inserted, and the server predicted the best structure prediction. The predicted structure was further refined through the Galaxy Refine server (<http://galaxy.seoklab.org/cgi-bin/submit.cgi?type=REFINE>). The PDB files generated from the RaptorX server were used as input. Then the result obtained was screened to obtain the ideal construct based on the Molprobit, and Rama favored the score. Furthermore, the refined structure was assessed by Ramachandran plot analysis using the SwissProt Expasy server (<https://swissmodel.expasy.org/assess>). Docking was then performed using the ClusPro plugin through PyMol. The utilized algorithm is the Lamarckian Genetic Algorithm (LGA) to check the binding affinity of the 3D structure and molecular docking.

5.7. Self-peptide Analysis

The peptide sequence of the vaccine construct was put into NCBI-BLASTp (<https://blast.ncbi.nlm.nih.gov/Blast.cgi?PAGE=Proteins>) to evaluate whether the peptide sequence exhibited similarities to human proteins. As such, the peptide vaccine sequence was compared with Homo sapiens (taxid:9606) in NCBI-BLASTp against the refseq protein database.

Acknowledgements: This study was not supported financially. The authors would like to thank the Research and Community Service Department (LPPM) of the Indonesia International Institute for Life Sciences (i3L) for their heartfelt support and providing the facilities for this research.

Author contributions: Concept – A., M.J., N.M.J.; Design – A., M.J., N.M.J.; Supervision – A.A.P.; Resources – A., M.J., N.M.J.; Materials – A., M.J., N.M.J.; Data Collection and/or Processing – A., M.J., N.M.J.; Analysis and/or Interpretation – A., M.J., N.M.J.; Literature Search – A., M.J., N.M.J.; Writing – A., M.J., N.M.J.; Critical Reviews – A., M.J., N.M.J., A.A.P.

Conflict of interest statement: The authors declared no conflict of interest.

REFERENCES

- [1] Sung H, Ferlay J, Siegel RL, Laversanne M, Soerjomataram I, Jemal A, et al. Global cancer statistics 2020: GLOBOCAN estimates of incidence and mortality worldwide for 36 cancers in 185 countries. *CA Cancer J Clin.* 2021; 71(3): 209–49. [Crossref]
- [2] Ringelhan M, McKeating JA, Protzer U. Viral hepatitis and liver cancer. *Philos Trans R Soc Lond B Biol Sci.* 2017; 372(1732): 20160274. [Crossref]
- [3] Long X-D, Deng Y, Huang X-Y, Yao J-G, Su Q-Y, Wu X-M, et al. Molecular Mechanisms of Hepatocellular Carcinoma Related to Aflatoxins: An Update. *Liver Research and Clinical Management.* Intech Open. 2017. [Crossref]
- [4] Marengo A, Rosso C, Bugianesi E. Liver Cancer: Connections with Obesity, Fatty Liver, and Cirrhosis. *Annu Rev Med.* 2016; 67(1): 103–17. [Crossref]
- [5] Forner A, Llovet JM, Bruix J. Hepatocellular carcinoma. *The Lancet.* 2012; 379(9822): 1245–55. [Crossref]
- [6] Ayoub WS, Steggerda J, Yang JD, Kuo A, Sundaram V, Lu SC. Current status of hepatocellular carcinoma detection: screening strategies and novel biomarkers. *Ther Adv Med Oncol.* 2019; 11:1758835919869120. [Crossref]
- [7] Patel N, Yopp AC, Singal AG. Diagnostic delays are common among patients with hepatocellular carcinoma. *J Natl Compr Canc Netw.* 2015;13(5):543–549. [Crossref]
- [8] Schütte K, Balbisi F, Malfertheiner P. Prevention of Hepatocellular Carcinoma. *Gastrointest Tumors.* 2016;3(1):37–43. [Crossref]
- [9] Raza A, Sood GK. Hepatocellular carcinoma review: current treatment, and evidence-based medicine. *World J Gastroenterol.* 2014;20(15):4115–4127. [Crossref]
- [10] Tsoulfas G, Agorastou P, Tooulias A, Marakis GN. Current and Future Challenges in the Surgical Treatment of Hepatocellular Carcinoma: A Review. *Int Surg.* 2014; 99(6): 779–86. [Crossref]
- [11] West H (Jack), Jin JO. Transarterial Chemoembolization. *JAMA Oncology.* 2015 Nov 1;1(8):1178. [Crossref]
- [12] Lahat, E., Eshkenazy, R., Zendel, A., Zakai, B. B., Maor, M., Dreznik, Y., & Ariche, A. Complications after percutaneous ablation of liver tumors: a systematic review. *Hepatobiliary Surg Nutr.* . 2014; 3(5), 317–323. [Crossref]
- [13] Faivre S, Rimassa L, Finn RS. Molecular therapies for HCC: Looking outside the box. *Journal of Hepatology.* 2020 Feb;72(2):342–52. [Crossref]
- [14] Lu L, Jiang J, Zhan M, Zhang H, Wang Q, Sun S, et al. Targeting Tumor-Associated Antigens in Hepatocellular Carcinoma for Immunotherapy: Past Pitfalls and Future Strategies. *Hepatology.* 2021 Feb;73(2):821–32. [Crossref]
- [15] Palata O, Podzimekova Hradilova N, Mysiková D, Kutna B, Mrazkova H, Lischke R, et al. Detection of tumor antigens and tumor-antigen specific T cells in NSCLC patients: Correlation of the quality of T cell responses with NSCLC subtype. *Immunology Letters [Internet].* 2020 Mar 1 [cited 2021 Jul 13];219:46–53. [Crossref]
- [16] Walesky C, Apte U. Mechanisms of Termination of Liver Regeneration. *Liver Regeneration.* 2015; 103–11.
- [17] Guo M, Zhang H, Zheng J, Liu Y. Glypican-3: A New Target for Diagnosis and Treatment of Hepatocellular Carcinoma. *J Cancer.* 2020; 11(8): 2008–21. [Crossref]
- [18] Wu Y, Liu H, Ding H. GPC-3 in hepatocellular carcinoma: current perspectives. *J Hepatocell Carcinoma.* 2016;3:63–67 [Crossref]
- [19] Kolluri A, Ho M. The Role of Glypican-3 in Regulating Wnt, YAP, and Hedgehog in Liver Cancer. *Front Oncol.* 2019;9. [Crossref]
- [20] Capurro M, Martin T, Shi W, Filmus J. Glypican-3 binds to Frizzled and plays a direct role in the stimulation of canonical Wnt signaling. *J Cell Sci.* 2014 Apr 1;127(7):1565–75. [Crossref]
- [21] Sawada Y, Yoshikawa T, Ofuji K, Yoshimura M, Tsuchiya N, Takahashi M, et al. Phase II study of the GPC3-derived peptide vaccine as an adjuvant therapy for hepatocellular carcinoma patients. *Oncoimmunology.* 2016; 5(5):e1129483. [Crossref]
- [22] Tada F, Abe M, Hirooka M, Ikeda Y, Hiasa Y, Lee Y, et al. Phase I/II study of immunotherapy using tumor antigen-pulsed dendritic cells in patients with hepatocellular carcinoma. *Int J Oncol.* 2012 Nov 1;41(5):1601–9. [Crossref]
- [23] Lee J-H, Tak WY, Lee Y, Heo M-K, Song J-S, Kim H-Y, et al. Adjuvant immunotherapy with autologous dendritic cells for hepatocellular carcinoma, randomized phase II study. *Oncoimmunology.* 2017;e1328335. [Crossref]

- [24] Pradana KA, Widjaya MA, Wahjudi M. Indonesians Human Leukocyte Antigen (HLA) Distributions and Correlations with Global Diseases. *Immuno Inves.* 2019; 49(3): 333–63. [[Crossref](#)]
- [25] Zhao L, Zhang M, Cong H. Advances in the study of HLA-restricted epitope vaccines. *Hum Vaccin Immunother.* 2013; 9(12):2566–77. [[Crossref](#)]
- [26] Cun Y, Li C, Shi L, Sun M, Dai S, Sun L, et al. COVID-19 coronavirus vaccine T cell epitope prediction analysis based on distributions of HLA class I loci (HLA-A, -B, -C) across global populations. *Hum Vaccin Immunother.* 2021 Apr 3;17(4):1097–108. [[Crossref](#)]
- [27] Farhood B, Najafi M, Mortezaee K. CD8 + cytotoxic T lymphocytes in cancer immunotherapy: A review. *Journal of Cellular Physiology.* 2018 Nov 22;234(6):8509–21. [[Crossref](#)]
- [28] St. Paul M, Ohashi PS. The roles of CD8+ T cell subsets in antitumor immunity. *Trends Cell Biol* 2020;30(9):695-704. [[Crossref](#)]
- [29] Castro F, Cardoso AP, Gonçalves RM, Serre K, Oliveira MJ. Interferon-Gamma at the Crossroads of Tumor Immune Surveillance or Evasion. *Front Immunol.* 2018 May 4;9. [[Crossref](#)]
- [30] Kinker G, Vitiello G, Ferreira W, Chaves A, Cordeiro de Lima V, Medina T. B Cell Orchestration of Anti-tumor Immune Responses: A Matter of Cell Localization and Communication. *Front Cell Dev Biol.* 2021;9. [[Crossref](#)]
- [31] Schwartz M, Zhang Y, Rosenblatt JD. B cell regulation of the anti-tumor response and role in carcinogenesis *J Immunother Cancer.* 2016;4:40. [[Crossref](#)]
- [32] Wang S, Liu W, Ly D, Xu H, Qu L, Zhang L. Tumor-infiltrating B cells: their role and application in anti-tumor immunity in lung cancer. *Cell Mol Immunol.* 2018 Apr 8;16(1):6–18. [[Crossref](#)]
- [33] Malonis RJ, Lai JR, Vergnolle O. Peptide-based vaccines: Current progress and future challenges. *Chem Rev.* 2019;120(6):3210–3229. [[Crossref](#)]
- [34] Nezafat N, Ghasemi Y, Javadi G, Khoshnoud MJ, Omidinia E. A novel multi-epitope peptide Vaccine against cancer: An in silico approach. *J Theor Biol.* 2014;349:121–134. [[Crossref](#)]
- [35] Quan, X., Sun, D., Zhou, J. Molecular Mechanism of HIV-1 TAT Peptide and its Conjugated Gold Nanoparticles Translocating across Lipid Membranes. *Phys Chem Chem Phys.* 2019;;21:10300– 10310. [[Crossref](#)]
- [36] Dong R, Chu Z, Yu F, Zha Y. Contriving multi-epitope subunit of vaccine for covid-19: Immunoinformatics approaches. *Front Immunol.* 2020;11. [[Crossref](#)]
- [37] Fishman JM, Wiles K, Wood KJ. The acquired immune system response to biomaterials, including both naturally occurring and synthetic biomaterials. *Host Response to Biomaterials.* 2015:151–187. [[Crossref](#)]
- [38] Wang S, Li W, Liu S, Xu J. RaptorX-Property: a web server for protein structure property prediction. *Nuc Acid Res.* 2016 Jul 8;44(W1):W430–435. [[Crossref](#)]
- [39] Buchan D, Jones D. The PSIPRED Protein Analysis Workbench: 20 years on. *Nucleic Acids Res.* 2019;47(W1):W402–W407. [[Crossref](#)]
- [40] Drozdetskiy A, Cole C, Procter J, Barton GJ. JPred4: a protein secondary structure prediction server. *Nucleic Acids Res.* 2015 Jul 1;43(W1):W389–394. [[Crossref](#)]
- [41] Faraggi E, Zhang T, Yang Y, Kurgan L, Zhou Y. SPINE X: Improving protein secondary structure prediction by multi-step learning coupled with prediction of solvent accessible surface area and backbone torsion angles. *J Comput Chem.* 2012 Jan 30;33(3):259–67. [[Crossref](#)]
- [42] Joo K, Lee SJ, Lee J. Sann: solvent accessibility prediction of proteins by nearest neighbor method. *Proteins.* 2012 Jul;80(7):1791–7. [[Crossref](#)]
- [43] Huang YJ, Mao B, Aramini JM, Montelione GT. Assessment of template based protein structure predictions in CASP10. *Proteins.* 2014 Feb;82(0 2):43–56. [[Crossref](#)]
- [44] Williams C, Headd J, Moriarty N, Prisant M, Videau L, Deis L et al. MolProbity: More and better reference data for improved all-atom structure validation. *Protein Sci.* 2017;27(1):293–315. [[Crossref](#)]
- [45] Chen K, Wu Z, Zhao H, Wang Y, Ge Y, Wang D, et al. XCL1/Glypican-3 Fusion Gene Immunization Generates Potent Antitumor Cellular Immunity and Enhances Anti-PD-1 Efficacy. *Cancer Immunol Res.* 2020 Jan;8(1):81–93. [[Crossref](#)]

- [46] Chauhan V, Rungta T, Goyal K, Singh MP. Designing a multi-epitope based vaccine to combat Kaposi Sarcoma utilizing immunoinformatics approach. *Sci Rep.* 2019 Feb 21;9:2517. [[Crossref](#)]
- [47] Abdelmoneim AH, Mustafa MI, Abdelmageed MI, Murshed NS, Dawoud E dk., Ahmed EM, et al. Immunoinformatics design of multiepitopes peptide-based universal cancer vaccine using matrix metalloproteinase-9 protein as a target. *Immunol Med.* 2021 Jan 2;44(1):35–52. [[Crossref](#)]
- [48] Kozakov D, Hall D, Xia B, Porter K, Padhorny D, Yueh C et al. The ClusPro web server for protein–protein docking. *Nat Protoc.* 2017;12(2):255-278. [[Crossref](#)]
- [49] Natasya, N., Tera, T., Savero, S., Swastika, N., & Parikesit, A. A. In silico computation of coagulation factor II: a potential water treatment agent against gram negative bacteria. *Note Sci Bio.* 2021; 13(1). [[Crossref](#)]
- [50] Igunnu A, Ambrose G, Adigun T. Mechanistic insight into the interactions between thiazolidinedione derivatives and PTP-1B combining 3D QSAR and molecular docking in the treatment of type 2 diabetes. *Physical Sciences Reviews.* 2020;0(0). [[Crossref](#)]
- [51] Qian S, Waldron L, Choudhary N, Klevit R, Chazin W, Patterson C. Engineering a Ubiquitin Ligase Reveals Conformational Flexibility Required for Ubiquitin Transfer. *J Biochem.* 2009;284(39):26797-26802. [[Crossref](#)]